Statistical mean-field approach to a disordered Hubbard model

1993 J. Phys.: Condens. Matter 5 1841

(http://iopscience.iop.org/0953-8984/5/12/012)

J. Phys.: Condens. Matter 5 (1993) 1841–1862. Printed in the UK

Statistical mean-field approach to a disordered Hubbard model

David E Logan and Fabio Siringo†
University of Oxford, Physical Chemistry Laboratory, South Parks Road, Oxford OX1 3QZ, UK

Received 11 June 1992, in final form 20 January 1993

Abstract. We develop a simple statistical mean-field treatment of a disordered Hubbard model. The presence of disorder, reflecting a range of local environments, may lead to local moment formation on an inhomogeneous scale; the essential element of the theory is a self-consistent description of local charges and magnetic moments on sites of different site energies, ϵ, arising from the occurrence of site disorder. The resultant theory is shown to be, in effect, a coupled infinite-component analogue of the single-impurity Anderson model, a helpful physical parallel in interpreting results from the theory. In addition to local charge and moment distributions, we consider self-consistently determined local and total pseudoparticle spectra, ϵ-dependent site occupation probabilities, and a measure of the Fermi-level charge distribution over the sites. Particular attention is given to the evolution of the interplay between disorder and interactions as the band filling fraction, y, is increased from $y \simeq 0$ through to the half-filled limit, $y = 1$, and to the differential influence of the Hubbard U on the local moment stability for different filling fractions.

1. Introduction

The interplay between disorder and electron interactions is a multifaceted problem of much current interest [1–18]. In this regard a one-band disordered Hubbard model is a rich and challenging model for study by a wide variety of methods [10–18]. The model Hamiltonian is

$$H = \sum_{i,\sigma} \epsilon_i n_{i\sigma} + \sum_{i,j,\sigma}{}' V_{ij} c_{i\sigma}^{\dagger} c_{j\sigma} + \tfrac{1}{2} U \sum_{i,\sigma} n_{i\sigma} n_{i-\sigma} \tag{1.1}$$

where the i/j sums run over all $N_s \to \infty$ sites with centre-of-mass positions $\{\boldsymbol{R}_i\}$, $\sigma = \pm$ denotes the spin, and $c_{i\sigma}^{\dagger}/c_{i\sigma}$ are the usual creation/annihilation operators with $n_{i\sigma} = c_{i\sigma}^{\dagger} c_{i\sigma}$ the σ-spin number operator for site i. On-site interactions are embodied in the repulsive Hubbard U. For site-disordered models, disorder occurs solely in the distribution of site energies, ϵ_i, usually regarded as independent random variables drawn from a common probability distribution $g(\epsilon)$ [12–15]; models with point-defect disorder leading to locally correlated random site energies are also important [10]. For topologically disordered Hubbard models [11, 16–18], in contrast, off-diagonal disorder in the distribution of one-electron hopping matrix elements

† Permanent address: Dipartimento di Fisica, Universita di Catania, Corso Italia 57, 95129 Catania, Italy.

0953-8984/93/121841+22$07.50

$V_{ij} \equiv V(|\boldsymbol{R}_i - \boldsymbol{R}_j|)$ is dominant, arising from disorder in the site centre-of-mass positions. In general, site-diagonal and off-diagonal disorder may each be operative to a variable extent.

An unrestricted Hartree–Fock (UHF) treatment is probably the simplest non-trivial approximation to a disordered Hubbard model. Although interactions are treated at a mean-field level, such an approach introduces the possibility of magnetism from the outset, and is thus important in describing the instability of the system to local moment formation [11, 19]. Further, since disorder leads to a range of local environments, local moment formation will thereby occur on an inhomogeneous scale [11]. Thus, while UHF is a mean-field approximation, it is so in a quantum sense for each disorder realization; and interesting statistical questions arise in describing, for example, the distribution of local charges and moments over the sites, with consequent effects for the single-particle spectra, localization of pseudoparticle states, etc.

We describe here a simple statistical mean-field approach [20] to some aspects of a disordered Hubbard model at a UHF level. The work is partly motivated by an interest in disordered charge-transfer binary alloys consisting of two s-band metals, one electropositive (C) and one electronegative (A): namely $C_xA_{1-x} \equiv C_y[CA]_{1-y}$ with $x = N_C/(N_C + N_A)$, and $y = (2x-1)/x = (N_C - N_A)/N_C$ the excess C-species fraction above the stoichiometric limit $x = \frac{1}{2}, y = 0$. The liquid Cs–Au alloy [21] is a relevant example, discussed in [22] and references therein. Insofar as the A band acts largely as an electron sink, the one-band Hamiltonian (1.1) is a useful caricature of the C-species conduction band for $x \geqslant \frac{1}{2}$, the sites representing 'active' C-species sites with $N_s = N_C$, $N_e = N_C - N_A$ the number of 'excess' electrons available to the C band, and $y = N_e/N_s$ the band filling fraction. The diagonal disorder, mimicked by a continuous $g(\epsilon)$, reflects Coulombic site disorder in the effective C-species site energies due to Coulomb interactions with the disordered distribution of surrounding ions, RMS fluctuations in which typically occur on an eV scale [22]. Topological disorder will also generate disorder in the $\{V_{ij}\}$ which enable electron hopping between active sites, but at the high number densities typical of, for example, Cs–Au this is likely to be of less significance. We thus view the site disorder, reflecting the distribution of local Coulombic environments for the active sites, as being of primary importance.

The basic mean-field equations are set up in section 2, the key element of which is a self-consistent determination, at a CPA level, of site-differential local charges and magnetic moments, together with relevant total and local disorder-averaged pseudoparticle spectra. Useful derivative quantities are also introduced, in particular the charge distribution for pseudoparticle states of energy E over the sites with site energies ϵ.

Some limits and connections of the theory should be mentioned. In the atomic limit $V_{ij} = 0$, and for any U and band filling y, it reproduces exactly the distribution of local charges and moment magnitudes over the sites, and the spin-summed total and local spectra. In the $g(\epsilon) = \delta(\epsilon)$ limit of no site-disorder, and at half-filling $y = 1$, it reduces essentially to Cyrot's [19] random field CPA treatment of the paramagnetic local moment phase of crystalline systems (see also Economou *et al* [23]). In section 3 we show further that the present theory may be viewed, in effect, as an infinite-component analogue of the single-impurity Anderson model [24], a parallel for which important numerical evidence has recently been found [11] in the context of a topologically disordered Hubbard model, and exploitation of which is helpful in interpreting results from the theory.

Detailed results are given in section 4, with emphasis on the variation with filling fraction y, from the empty band limit $y = 0$ (which is, equivalently, the non-interacting limit) through to half-filling, $y = 1$. Three qualitatively distinct y regimes are identified—quasiatomic, intermediate and non-magnetic domains—and their characteristics, which stem from the interplay between disorder and interaction effects, are described. In section 5 the role of varying U is examined, with particular attention paid to the differential influence of the interaction strength on local moment stability for different filling fractions.

2. Theory

For any disorder realization, the familiar 'Ising-spin' UHF Hamiltonian is

$$H = \sum_{i,\sigma} \epsilon_{i\sigma} n_{i\sigma} + \sum_{i,j,\sigma}{}' V_{ij} c_{i\sigma}^{\dagger} c_{j\sigma} \equiv \sum_{\sigma} H_{\sigma}. \tag{2.1}$$

The site σ-spin Green functions are defined by

$$G_{ij;\sigma}(E) = \langle 0 | c_{i\sigma} (E + i\eta - H_{\sigma})^{-1} c_{i\sigma}^{\dagger} | 0 \rangle$$

with $\eta \to 0+$. In (2.1) the effective σ-spin site energy $\epsilon_{i\sigma}$ is given by

$$\epsilon_{i\sigma} = \epsilon_i + U \bar{n}_{i-\sigma} = \epsilon_i + \tfrac{1}{2} U [n_i - \sigma \mu_i]. \tag{2.2}$$

The overbar denotes an expectation value over the UHF ground state, and the site local charge (n_i) and magnetic moment (μ_i) are given respectively by $n_i / \mu_i = \bar{n}_{i+} \pm \bar{n}_{i-}$. Two sources of 'pure' disorder are in general assumed to be present: off-diagonal disorder in the $\{V_{ij}\}$ (arising from topological disorder in the $\{\boldsymbol{R}_i\}$); and, of central importance, disorder in the bare site energies $\{\epsilon_i\}$. These are regarded as independent random variables with a common distribution $g(\epsilon)$, assumed to be continuous and symmetric, with upper/lower edges at ϵ_{U} and $\epsilon_{\mathrm{L}} = -\epsilon_{\mathrm{U}}$.

Disorder in the σ-spin site energies $\{\epsilon_{i\sigma}\}$ that enter H_{σ}, arises both from explicit disorder in the bare $\{\epsilon_i\}$ and from charge and spin disorder in the distribution of $\{n_i, \mu_i\}$. A full determination of $\{n_i, \mu_i\}$ is a detailed question of self-consistency, but any approximate theory for a disordered system must clearly allow, at some self-consistent level, for site-differential local charges/moments. Charge fluctuations in this sense are particularly important for, since $|\mu_i| \leqslant \min(n_i, 2 - n_i)$, their existence cannot be divorced from the question of site-differential local moment stability, and may strongly enhance the role of interactions in leading to local moment formation. At low filling fractions $y \to 0$, for example, we envisage the possibility of $n_i \simeq 0$ on most sites but $n_i \simeq 1$ on a few, corresponding to strong localization of the occupied pseudoparticle states in the vicinity of low-ϵ_i sites, with enhancement of interactions due to charge localization leading to strong moments on the significantly occupied sites [20, 22]. Such a possibility clearly cannot be described if charge fluctuations are entirely neglected, as this corresponds to setting $n_i = y \simeq 0$ for all sites. It is further clear that ϵ_i itself is central in determining the self-consistent n_i and $|\mu_i|$: for example, in the atomic limit $\{V_{ij}\} = 0$, these are determined uniquely by the value of ϵ_i, with $n_i = 0, 1$ or 2 according to site occupancy, and $|\mu_i| = \min(n_i, 2 - n_i)$.

The basic physical idea of the present theory is to use the bare ϵ's as a 'window' on local environments, and to allow for site-differential local charges, moments and local moment (or spin) fluctuations, determined self-consistently at a CPA level, and embodied in a conditional probability density $P(n_i;\mu_i|\epsilon)$ common to all sites with a *given* site energy $\epsilon_i = \epsilon$, which is chosen to reproduce correctly the atomic limit; details are given below. The existence, or otherwise, of ϵ-differential local moments is thus deemed to be of primary importance, spatial correlation between the n_i/μ_i on different sites being neglected and the $\{\epsilon_{i\sigma}\}$ thus regarded as independent random variables. While such an approach is simple it can, we believe, capture important broad features of the interplay between disorder and interaction effects; see also [25,26] for computational studies that support this view.

2.1. *Basic mean-field equations*

With $\langle\cdots\rangle$ denoting a full disorder average, the averaged total density of single-particle excitations (DOS) $D(E) = \frac{1}{2}\sum_\sigma D_\sigma(E)$; and the total σ-spin DOS $D_\sigma(E) = -\pi^{-1}\mathrm{Im}\bar{G}_\sigma(E)$ is obtained from $\bar{G}_\sigma(E) = \langle N_s^{-1}\sum_i G_{ii;\sigma}(E)\rangle(\equiv \langle G_{ii;\sigma}(E)\rangle)$. With the above approximations $\bar{G}_\sigma(E)$ may be written formally as

$$\bar{G}_\sigma(E) = \int F(\epsilon_{i\sigma})\bar{G}_\sigma(\epsilon_{i\sigma};E)\mathrm{d}\epsilon_{i\sigma} \tag{2.3}$$

where $F(\epsilon_{i\sigma})$ is the distribution of σ-spin site energies, and $\bar{G}_\sigma(\epsilon_{i\sigma};E)$ is a disorder average of $G_{ii;\sigma}$ in which $\epsilon_{i\sigma}$ is constrained. This takes the form (see, for example, [27])

$$\bar{G}_\sigma(\epsilon_{i\sigma};E) = \left(E + \mathrm{i}\eta - \epsilon_{i\sigma} - \Sigma_\sigma(E)\right)^{-1} \tag{2.4}$$

where the improper self-energy is thus defined. Within the framework of any single-site theory (such as CPA [28,29], EMA [30] or SSCA/MSA [31]) $\Sigma_\sigma(E) \equiv \Sigma(\bar{G}_\sigma(E))$, i.e. is independent of $\epsilon_{i\sigma}$ and a specified function solely of $\bar{G}_\sigma(E)$; see, for example, [27].

With $F(\epsilon_{i\sigma})$ specified, (2.3) and (2.4) enable a self-consistent determination of $\bar{G}_\sigma(E)$. The function $F(\epsilon_{i\sigma})$ is of the form

$$F(\epsilon_{i\sigma}) = \int \mathrm{d}\epsilon \int \mathrm{d}n_i \int \mathrm{d}\mu_i g(\epsilon)P(n_i;\mu_i|\epsilon)\delta(\epsilon_{i\sigma} - [\epsilon + \tfrac{1}{2}U(n_i - \sigma\mu_i)]) \tag{2.5}$$

where P is the (normalized) conditional distribution for n_i, μ_i as above. With (2.5), equation (2.3) yields

$$\bar{G}_\sigma(E) = \int_{-\infty}^{\infty} \bar{G}_\sigma(\epsilon;E)g(\epsilon)\mathrm{d}\epsilon \tag{2.6}$$

where $\bar{G}_\sigma(\epsilon;E)$ is given by

$$\bar{G}_\sigma(\epsilon;E) = \int \mathrm{d}n_i \int \mathrm{d}\mu_i P(n_i;\mu_i|\epsilon)\bar{G}_\sigma(\epsilon_{i\sigma};E) \tag{2.7}$$

and is a disorder average of the diagonal Green function for sites with a given $\epsilon_i = \epsilon$, in which only the *bare* site energy ϵ is thus constrained: $\bar{G}_\sigma(\epsilon;E) =$

$\langle N_\epsilon^{-1} \sum_{i:\epsilon_i=\epsilon} G_{ii;\sigma} \rangle$, with N_ϵ the number of sites with $\epsilon_i = \epsilon$ such that $N_\epsilon/N_s = g(\epsilon)\mathrm{d}\epsilon$; the corresponding local DOS, $D_\sigma(\epsilon; E)$, will be discussed further below.

For $P(n_i; \mu_i|\epsilon)$ we use in practice the model form

$$P(n_i; \mu_i|\epsilon) = \delta(n_i - n(\epsilon))\tfrac{1}{2}[\delta(\mu_i - |\mu(\epsilon)|) + \delta(\mu_i + |\mu(\epsilon)|)] \quad (2.8)$$

with $n(\epsilon) = \langle N_\epsilon^{-1} \sum_{i:\epsilon_i=\epsilon} n_i \rangle$ the mean charge per site of energy ϵ and $|\mu(\epsilon)|$ the corresponding mean magnitude of the site local moment, which are determined self-consistently via (2.13). Charge fluctuations are thus introduced via an ϵ-differential $n(\epsilon)$, while being neglected for sites with the same site energies (as is exact in the atomic limit). Likewise, for sites with $\epsilon_i = \epsilon$, $\mu_i = \pm|\mu(\epsilon)|$ with equal probability, reflecting ϵ-differential spin fluctuations corresponding to an assumed paramagnetic local moment state. There are two physical ways to view the local moment distribution, between which the present theory does not discriminate: either as a frozen spin-glass-like local moment state (as found in $T = 0$ numerical studies at the UHF level [25,26]); or, following Cyrot [19], as providing a snapshot of a dynamically fluctuating paramagnetic local moment distribution above any relevant magnetic ordering temperature (as would be appropriate, for example, to liquid Cs–Au). Note that (2.8) implies the obvious up–down spin symmetry $F(\epsilon_{i\sigma}) = F(\epsilon_{i-\sigma})$, and

$$\bar{G}_\sigma(\epsilon; E) = \bar{G}_{-\sigma}(\epsilon; E) \quad \bar{G}_\sigma(E) = \bar{G}_{-\sigma}(E) \quad \Sigma_\sigma(E) = \Sigma(\bar{G}_\sigma(E)) = \Sigma_{-\sigma}(E). \quad (2.9)$$

From (2.8), (2.7) and (2.4), $\bar{G}_\sigma(E)$ may be written as

$$\bar{G}_\sigma(\epsilon; E) = \tfrac{1}{2}[\bar{G}_\sigma^{(\sigma)}(\epsilon; E) + \bar{G}_\sigma^{(-\sigma)}(\epsilon; E)] \quad (2.10a)$$

with

$$\bar{G}_\sigma^{(\pm\sigma)}(\epsilon; E) = [E + \mathrm{i}\eta - \epsilon_\sigma^{(\pm\sigma)} - \Sigma(\bar{G}_\sigma(E))]^{-1} \quad (2.10b)$$

and

$$\epsilon_\sigma^{(\pm\sigma)} = \epsilon + \tfrac{1}{2}U[n(\epsilon) \mp |\mu(\epsilon)|] \quad (2.11a)$$

$$\equiv \epsilon + U n_{-\sigma}^{(\pm\sigma)}(\epsilon). \quad (2.11b)$$

Physically, $\bar{G}_\sigma^{(\sigma')}(\epsilon; E)$ is the averaged σ-spin Green function for those sites of energy ϵ (half the total of such) that are preferentially occupied by σ'-spin electrons and thus have local moments $\mu(\epsilon) = \sigma'|\mu(\epsilon)|$; and for which the effective σ-spin site energy $\epsilon_\sigma^{(\sigma')} (= \epsilon_{-\sigma}^{(-\sigma')})$ is (2.11), with $n_{-\sigma}^{(\sigma')}$ the mean number of $-\sigma$-spin electrons on such sites. Clearly

$$\bar{G}_\sigma^{(\sigma')}(\epsilon; E) = \bar{G}_{-\sigma}^{(-\sigma')}(\epsilon; E) \quad (2.12)$$

and similarly for the corresponding DOS, $D_\sigma^{(\sigma')}(\epsilon; E)$. In terms of these, the appropriate self-consistency equations for $n(\epsilon)$ and $|\mu(\epsilon)|$ are

$$n(\epsilon) = \int_{-\infty}^{E_F} \sum_\sigma D_\sigma^{(\sigma')}(\epsilon; E)\mathrm{d}E \qquad (\mu(\epsilon) \equiv)\ \sigma'|\mu(\epsilon)| = \int_{-\infty}^{E_F} \sum_\sigma \sigma D_\sigma^{(\sigma')}(\epsilon; E)\mathrm{d}E \quad (2.13)$$

and are independent of σ', being invariant under $\sigma' \leftrightarrow -\sigma'$.

With $\Sigma(E) \equiv \Sigma(\bar{G}_\sigma(E))$ specified as a function of $\bar{G}_\sigma$, the essential mean-field self-consistency equations are (2.6) and (2.10) for $\bar{G}_\sigma(E)$, and (2.13) for $n(\epsilon)/|\mu(\epsilon)|$; the two sets are clearly coupled via the dependence of $\bar{G}_\sigma^{(\sigma')}(\epsilon; E)$ on ϵ, E and $\bar{G}_\sigma(E)$. The solution of these equations, together with simple number conservation

$$y = \int_{-\infty}^{E_F} n(\epsilon) g(\epsilon) \mathrm{d}\epsilon = 2 \int_{-\infty}^{E_F} D(E) \mathrm{d}E \tag{2.14}$$

(stemming from $y = N_s^{-1} \sum_i n_i$), enables a complete determination of $n(\epsilon), |\mu(\epsilon)|$, the relevant DOS and the Fermi energy $E_F = E_F(y)$. The model $P(n_i; \mu_i|\epsilon)$, equation (2.8), is the simplest choice enabling a correct description of the atomic limit, for which $n(\epsilon), |\mu(\epsilon)|$, $D(E)$ and $D(\epsilon; E) = \frac{1}{2}\sum_\sigma D_\sigma(\epsilon; E)$ are reproduced exactly by the theory. In addition, for the $U = 0$ non-interacting limit, $\epsilon_{i\sigma} = \epsilon_i$; the distribution P is then irrelevant, $F(\epsilon_{i\sigma})$ reduces to $g(\epsilon)$, and the only inherent approximation is a single-site theory for the averaged Green functions.

For the specific results of section 4 we employ a cut Lorentzian $g(\epsilon)$, and the simplest, so-called Hubbard, approximation [32] for $\Sigma(\bar{G}_\sigma)$, namely

$$\Sigma(\bar{G}_\sigma) = J_2 \bar{G}_\sigma \tag{2.15}$$

with $J_2 = \langle \sum_j' |V_{ij}|^2 \rangle$. It is straightforward to show that (2.15) satisfies the CPA condition [28, 29] for the site disorder, with a reference semi-elliptic spectrum $D_0(E)$ (appropriate to the unperturbed limit $g(\epsilon) = \delta(\epsilon)$, $U = 0$ of no site disorder or interactions), namely

$$D_0(E) = [4J_2 - E^2]^{1/2}/2\pi J_2 \qquad E^2 \leqslant 4J_2 \tag{2.16a}$$

with a full bandwidth

$$B = 4J_2^{1/2} \tag{2.16b}$$

determined via J_2, which is in turn easily related to the number density of active sites, ρ, and to structural parameters of the system, see e.g. [27].

2.2. *Derivative properties*

The following quantities follow directly from solution of the mean-field equations, and will be useful in interpreting the results of section 4.

(i) For any disorder realization, the eigenstates $|\Psi_{\alpha\sigma}\rangle$ of the UHF H_σ may be expanded in a site spin-orbital basis, $|\Psi_{\alpha\sigma}\rangle = \sum_i a_{i\alpha\sigma}|\phi_{i\sigma}\rangle$. The quantum probability that a σ-spin electron in a given state of energy $E_{\alpha\sigma}$ will be found on any of the sites with site energy ϵ is $p(\epsilon; E_{\alpha\sigma}) = \sum_{i:\epsilon_i=\epsilon} |a_{i\alpha\sigma}|^2$. Thus

$$h_\sigma(\epsilon; E)\mathrm{d}\epsilon = \frac{\sum_\alpha p(\epsilon; E_{\alpha\sigma})\delta(E - E_{\alpha\sigma})}{\sum_\alpha \delta(E - E_{\alpha\sigma})}$$

is the mean probability that a σ-spin electron in any of the σ-spin pseudoparticle states of energy E will be found on sites with $\epsilon_i = \epsilon$; equivalently, this is the mean fraction of charge in σ-spin states of energy E that will be found on such sites.

The corresponding disorder-averaged probability density, $H_\sigma(\epsilon; E) = \langle h_\sigma(\epsilon; E)\rangle$, is readily shown to reduce to

$$H_\sigma(\epsilon; E) = g(\epsilon) D_\sigma(\epsilon; E)/D_\sigma(E). \tag{2.17}$$

By definition, $\int d\epsilon H_\sigma(\epsilon; E) = 1$, and from (2.9) $H_\sigma = H_{-\sigma}$, reflecting the assumed paramagnetic local moment distribution. Although neither $h_\sigma(\epsilon; E)$ nor $H_\sigma(\epsilon; E)$ give direct information on Anderson localization of pseudoparticle states, they give a revealing measure of the charge distribution over sites for states of any given energy; $H_\sigma(\epsilon; E_F)$ for Fermi-level states will be considered in section 4.

(ii) Relatedly, the disorder averaged fraction of net ground-state charge found on sites of energy ϵ is $I(\epsilon)d\epsilon$, with the corresponding density given by $I(\epsilon) = g(\epsilon)n(\epsilon)/y$.

(iii) With $C(n)dn$ the disorder-averaged fraction of sites with ground-state charge between n and $n + dn$, $C(n) = \langle N_s^{-1} \sum_i \delta(n_i - n)\rangle$. From (2.8), $n_i = n(\epsilon)$ for all i with $\epsilon_i = \epsilon$, so

$$C(n) = \int_{-\infty}^{\infty} \delta(n - n(\epsilon)) g(\epsilon) d\epsilon. \tag{2.18}$$

(iv) For any disorder realization, $P_{mi}(m = 0, 1, 2)$ is the probability that site i is m-fold occupied by electrons in the ground state: $P_{2i} = \overline{n_{i+} n_{i-}} (= \frac{1}{4}(n_i^2 - \mu_i^2)$ in UHF), and P_{1i}, P_{0i} follow from charge and probability conservation, $\sum_m m P_{mi} = n_i$ and $\sum_m P_{mi} = 1$ respectively. Corresponding disorder-averaged site occupation probabilities follow, $P_m(\epsilon) = \langle N_\epsilon^{-1} \sum_{i:\epsilon_i = \epsilon} P_{mi}\rangle$, with

$$P_2(\epsilon) = \tfrac{1}{4}[n^2(\epsilon) - \mu^2(\epsilon)] \tag{2.19a}$$

and $P_1(\epsilon), P_0(\epsilon)$ obtained via

$$\sum_m P_m(\epsilon) = 1 \qquad \sum_m m P_m(\epsilon) = n(\epsilon). \tag{2.19b}$$

3. Multicomponent impurity analogue

We now highlight further the interpretation of some basic equations from the previous sections, and find and exploit a helpful physical parallel to the single-impurity Anderson model [24] (SIAM).

From the spin symmetries of (2.9) and (2.12), the total DOS $D(E) = \frac{1}{2}\sum_\sigma D_\sigma(E)$ is given from (2.6) by

$$D(E) = \int_{-\infty}^{\infty} D(\epsilon; E) g(\epsilon) d\epsilon \tag{3.1a}$$

$$= \int_{-\infty}^{\infty} \tfrac{1}{2}[D_\sigma^{(\sigma)}(\epsilon; E) + D_{-\sigma}^{(\sigma)}(\epsilon; E)] g(\epsilon) d\epsilon \tag{3.1b}$$

with $D(\epsilon;E)=\frac{1}{2}\sum_\sigma D_\sigma(\epsilon;E)$. Separating $\Sigma(\bar{G}_\sigma)=\Sigma(E)$ formally as $X(E)-\mathrm{i}\Delta(E)$, the $D^{(\sigma)}_{\sigma'}(\epsilon;E)$ in (3.1b) are given from (2.10b) by

$$D^{(\sigma)}_{\sigma'}(\epsilon;E)=\frac{\Delta(E)\pi^{-1}}{\left(E-\epsilon^{(\sigma)}_{\sigma'}-X(E)\right)^2+\Delta^2(E)} \tag{3.2}$$

with $\epsilon^{(\sigma)}_{\pm\sigma}=\epsilon+\frac{1}{2}U[n(\epsilon)\mp|\mu(\epsilon)|]$. The total DOS at energy E is thus a composite of the local $D(\epsilon;E)=\frac{1}{2}[D^{(\sigma)}_{\sigma}(\epsilon;E)+D^{(\sigma)}_{-\sigma}(\epsilon;E)]$ for sites of different ϵ. And the physical interpretation of $D^{(\sigma)}_{\sigma}/D^{(\sigma)}_{-\sigma}$ is clear: if sites of energy ϵ possess local moments, $|\mu(\epsilon)|>0$, then $D^{(\sigma)}_{\sigma}(\epsilon;E)$ and $D^{(\sigma)}_{-\sigma}(\epsilon;E)$ do not coincide and correspond respectively to lower and upper Hubbard subbands in the local spectrum; in contrast, if $|\mu(\epsilon)|=0$, whence $\epsilon^{(\sigma)}_{\sigma}=\epsilon+\frac{1}{2}Un(\epsilon)=\epsilon^{(\sigma)}_{-\sigma}$, then $D^{(\sigma)}_{\sigma}=D^{(\sigma)}_{-\sigma}$ and the local Hubbard bands 'collapse' together.

A full numerical solution of the mean-field self-consistency equations will be given in section 4, but it is useful here to make one further approximation, neglecting the E-dependence of $\Sigma(E)$ and writing $\Sigma(E)\simeq\Sigma(E_\mathrm{F})=X-\mathrm{i}\Delta(E_\mathrm{F})$. From (3.2) the local Hubbard bands $D^{(\sigma)}_{\pm\sigma}(\epsilon;E)$ for any ϵ then reduce to pure Lorentzians in E, centred on $E=\epsilon^{(\sigma)}_{\pm\sigma}(\epsilon)-X$ respectively and thus separated in energy by $U|\mu(\epsilon)|$, each having a width $\Delta(E_\mathrm{F})$. Using (2.15), for example, the width

$$\Delta(E_\mathrm{F})=\pi J_2 D(E_\mathrm{F}) \tag{3.3}$$

thus depends on the total Fermi-level DOS. With $\Sigma(E)\simeq\Sigma(E_\mathrm{F})$, the self-consistency equations for $n(\epsilon)$ and $|\mu(\epsilon)|$ at any ϵ, given generally by

$$\left.\begin{matrix}n(\epsilon)\\|\mu(\epsilon)|\end{matrix}\right\}=\int_{-\infty}^{E_\mathrm{F}}[D^{(\sigma)}_{\sigma}(\epsilon;E)\pm D^{(\sigma)}_{-\sigma}(\epsilon;E)]\mathrm{d}E \tag{3.4}$$

are then uncoupled from those for $\epsilon'\neq\epsilon$; and viewed as a function of $E_\mathrm{F}(y)$ and $\Delta(E_\mathrm{F})$ they are identical to those of the SIAM at the UHF level [24] for a single impurity with site energy $\epsilon_\mathrm{imp}=\epsilon$ (see equation (26) of [24]). Since we consider a continuous distribution of site energies, our mean-field theory for the disordered Hubbard model may, in effect, be viewed as an infinite-component analogue of the SIAM, an individual component being the set of sites with a given site energy ϵ. Such a parallel seems reasonable in general: for example, Milovanović and co-workers [11] recently examined the weak disorder instability of a disordered Fermi liquid to local moment formation, via a numerical study at a HF-type level of a topologically disordered Hubbard model, and found thereby a generalization of the SIAM compensation theorem [24].

With $\Sigma(E)\simeq\Sigma(E_\mathrm{F})$, and in a precise parallel to the SIAM [24], the value of ϵ relative to $E_\mathrm{F}(y)$ determines whether, for given $\Delta(E_\mathrm{F})/U$, sites with any given site energy possess local moments; and as $\Delta(E_\mathrm{F})/U=\pi J_2 D(E_\mathrm{F})/U$ increases, local moments will typically persist in a progressively smaller ϵ-interval. Thus, at low filling fractions y where $D(E_\mathrm{F})$ and hence $\Delta(E_\mathrm{F})$ is small, the local spectra $D^{(\sigma)}_{\pm\sigma}(\epsilon;E)$ (3.2) have narrow Anderson-like resonances, and strong local moments on a small fraction of low-ϵ sites are readily sustained. With increasing y, $D(E_\mathrm{F})$ and hence $\Delta(E_\mathrm{F})$ increase, and we thus anticipate the possibility of a threshold $y=y_0<1$

above which the system is nowhere unstable to local moment condensation: with site-disorder present, the effects of interactions, while insufficient to produce moments at half-filling $y = 1$, may nevertheless lead to strong local moment formation at low y; see sections 4 and 5.

More importantly, the SIAM parallel provides insight into the charge density (over sites) of pseudoparticle states, at E_F in particular. Consider a filling fraction y in a local moment regime, and let ϵ_m pertain to sites on which local moments $|\mu(\epsilon_m)|$ are a maximum. With $\Sigma(E) \simeq \Sigma(E_F)$ the centres of the Lorentzian Hubbard subbands in $D(\epsilon_m; E)$ are separated in E by $U|\mu(\epsilon_m)|$; and E_F must lie precisely midway between these centres, since from (3.4) for $|\mu(\epsilon)|$ the moment will decrease if E_F occurs at a lower or higher value. From (3.4) for $n(\epsilon)$, it follows that $n(\epsilon_m) = 1$. (With the E dependence of $\Sigma(E)$ restored the equality will not be strict, but we certainly expect $n(\epsilon_m) \simeq 1$ for those sites with maximum moments, see section 4.) Three points follow.

(i) The larger the local moment $|\mu(\epsilon_m)|$ is, the smaller the contribution made by sites with $\epsilon \simeq \epsilon_m$ to the local Fermi-level DOS, $D(\epsilon; E_F)$. Thus, sites with strong local moments typically give a relatively small contribution to the Fermi-level charge density $H_\sigma(\epsilon; E_F) \propto D_\sigma(\epsilon; E_F) \equiv D(\epsilon; E_F)$ (see (2.17)), and hence participate only weakly in Fermi-level pseudoparticle states. There is thus in effect only relatively weak overlap between the charge-carrying Fermi-level *states* and strong local moment *sites*, redolent of the assumptions that underly phenomenological two-fluid models (see e.g. [9,33]).

(ii) That $n(\epsilon_m) = 1$, as above, is independent of the magnitude of $|\mu(\epsilon_m)|$. If local moments (anywhere) have just stabilized, so $|\mu(\epsilon_m)|$ is small, then $D(\epsilon_m; E_F)$ will be significant due to substantial overlap of the Hubbard subbands in $D(\epsilon; E_F)$. Thus, when local moments can first be supported, the sites on which they have just stabilized (and for which $\epsilon_\sigma^{(\sigma)} \lesssim \epsilon + \frac{1}{2}U \lesssim \epsilon_{-\sigma}^{(\sigma)}$) will contribute appreciably to the Fermi-level charge density $H_\sigma(\epsilon; E_F)$. They will thus participate significantly in pseudoparticle states at E_F, as found in practice by Milovanović and co-workers [11].

(iii) In the non-magnetic domain, $|\mu(\epsilon)| = 0 \forall \epsilon$, $\epsilon_\sigma^{(\sigma)} = \epsilon + \frac{1}{2}Un(\epsilon) = \epsilon_{-\sigma}^{(\sigma)}$; $D(\epsilon; E)$ is then a single Lorentzian in E, centred on $E = \epsilon + \frac{1}{2}Un(\epsilon) - X$. Sites for which $\epsilon + \frac{1}{2}Un(\epsilon) - X = E_F$ will clearly contribute appreciably to $D(\epsilon; E_F)$, and from (3.4) have $n(\epsilon) = 1$. Thus, in the non-magnetic regime, $H(\epsilon; E_F)$ will again (as in (ii) above) receive a significant contribution from sites for which $n(\epsilon) \simeq 1$, whose effective site energies are close to $\epsilon + \frac{1}{2}U$.

Examples of the above, and further parallels to the SIAM [24], will be seen in the following sections.

4. Results: three y-domains

We now consider specific results obtained from the mean-field equations (2.6), (2.10) and (2.13). Equation (2.15) for $\Sigma(\tilde{G}_\sigma)$ is used, specified in terms of the full width B of the unperturbed ($U = 0, g(\epsilon) = \delta(\epsilon)$) DOS, $D_0(E)$ (equation (2.16)), which is illustrated in figure 1(a).

The basic features desired in $g(\epsilon)$ are also illustrated in figure 1(a), and may be motivated by the $C_xA_{1-x} \equiv C_y[CA]_{1-y}$ binary monovalent liquid alloy of section 1; see also [22]. For such, $g(\epsilon)$ mimics Coulombic site disorder in the electropositive C-species site energies, arising from the random Madelung potentials [22] characteristic

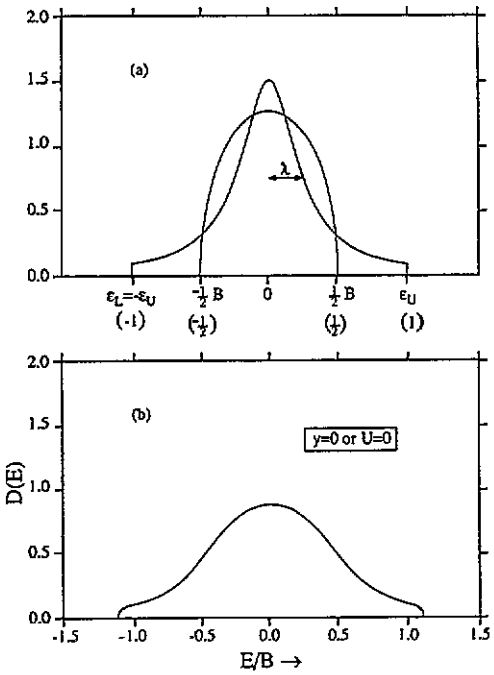

Figure 1. (*a*) The model site energy distribution $g(\epsilon)$ of halfwidth λ; and the zero-order DOS $D_0(E)$ of full width B. The B-scaled energies used in practice are shown in parenthesis. (*b*) Self-consistently determined DOS $D(E)$ for the non-interacting limit $\tilde{U} = 0$ (with $\tilde{\lambda} = 0.25$). Equivalently, this is $D(E)$ in the $y = 0$ empty-band limit for any $\tilde{U}$.

of the liquid alloy. At stoichiometry, $y = 0$, where the C-species conduction band is empty, $D_0(E)$ then models the zero-order conduction band, with $g(\epsilon) = \delta(\epsilon)$ corresponding to suppression of Coulombic site disorder as appropriate to the crystalline stoichiometric alloy. The Coulombic site disorder is effectively introduced by melting the crystalline alloy, and may lead [22,34] to a marked reduction in and smearing out of the optical gap for transitions to the conduction (C-species) band from the filled valence (A-species) band.

As illustrated in figure 1(*a*), we thus include a tail in the model $g(\epsilon)$ extending below the lower edge of the zero-order $D_0(E)$, with a width λ reflecting fluctuations in the Coulombic site disorder. With the C-species composition increased above stoichiometry, $y = 0$, the 'excess' electrons available to populate the conduction band will experience the localizing effects of the Coulombic site disorder mimicked by $g(\epsilon)$. In reality, λ will vary with y [22], but since we are not concerned here with particular system modelling we simply regard λ as the essential parameter for $g(\epsilon)$.

Specifically, we choose for $g(\epsilon)$ a cut Lorentzian of halfwidth λ, non-zero for $\epsilon_L = -\epsilon_U < \epsilon < \epsilon_U$ (a Gaussian $g(\epsilon)$ produces identical qualitative results). Provided $\epsilon_L < -\frac{1}{2}B$ the choice of cutoff in $g(\epsilon)$ is largely immaterial to us, and a fraction

$$y_c = \int_{\epsilon_L}^{-\frac{1}{2}B} g(\epsilon)\mathrm{d}\epsilon \tag{4.1}$$

of sites have site energies lying below the lower edge of $D_0(E)$, with y_c controlled by λ such that $y_c \to 0$ as $\lambda \to 0$.

The mean-field equations are thus characterized by the parameters U, B, λ and ϵ_U. In the atomic limit ($B \to 0$), $n(\epsilon), |\mu(\epsilon)|, D(E), D(\epsilon; E)$ and $C(n)$ are reproduced exactly by the theory for all U and y. Here we focus on $B > 0$ and scale all energies by B. The essential model parameters are thus

$$\tilde{U} = U/B \qquad \tilde{\lambda} = \lambda/B \tag{4.2}$$

and $\tilde{\epsilon}_U = \epsilon_U/B$ which for convenience we choose to be unity; corresponding B-scaled energies are shown in figure 1(*a*).

We consider first, for fixed $\tilde{U}$ and $\tilde{\lambda}$, the evolution with filling fraction up to half-filling $y = 1$ (since $D_0(E)$ and $g(\epsilon)$ are each symmetric, $y \leftrightarrow 2 - y$ particle–hole symmetry occurs). We choose $\tilde{\lambda} = 0.25$, so that a small fraction $y_c \simeq 0.08$ of sites have $\epsilon < -\frac{1}{2}B$, and a relatively weak coupling value of the scaled interaction strength, $\tilde{U} = \frac{1}{2}$—as is roughly appropriate to $Cs_y[CsAu]_{1-y}$ close to stoichiometry [20].

4.1. Quasiatomic regime, $y \lesssim y_c$

Figure 1(*b*) shows the self-consistently determined total DOS, $D(E)$, for the empty band limit $y = 0$; equivalently, this is just the non-interacting ($U = 0$) $D(E)$ for the disordered tight-binding model (TBM) to which the disordered Hubbard model reduces for $U = 0$.

On physical grounds we would expect TBM states towards the lower-energy edge of the $U = 0$ (or $y = 0$) $D(E)$—those below the lower edge at $E = -\frac{1}{2}B$ of the unperturbed $D_0(E)$—to be Anderson localized due to the site disorder, and to be associated primarily with low-ϵ sites: such sites are typically well separated in space, and surrounded by sites with higher ϵ such that $\Delta\epsilon$ is large compared to the hopping matrix elements that connect them.

This in turn will affect significantly the behaviour of the interacting system as the filling fraction is initially increased from $y = 0$. The mean separation between the electrons is $r_e \sim (y\rho_s)^{-1/3}$ with ρ_s the site number density. If U is sufficiently large, and the localization lengths ξ_λ of low-energy TBM states of energy E_λ are smaller than r_e, a double exclusion principle will in effect operate at sufficiently small y, whereby the ground state of the interacting $U > 0$ system consists essentially of a narrow energy range of mainly non-overlapping and singly occupied TBM states. As discussed in [22] (see also [16]), the limiting case of strictly non-overlapping singly occupied localized states can be described via a canonical transformation of the disordered Hubbard Hamiltonian to a representation in terms of basic operators $c^\dagger_{\lambda\sigma}/c_{\lambda\sigma}$ pertaining to the $U = 0$ TBM limit, followed by neglect of matrix elements (such as interstate spin-flip terms) involving on-site overlap of different TBM states. This leads to

$$H \simeq \sum_{\lambda,\sigma} E_\lambda n_{\lambda\sigma} + \frac{1}{2}\sum_{\lambda,\sigma} U_\lambda n_{\lambda\sigma} n_{\lambda-\sigma} \tag{4.3}$$

where $U_\lambda = UL(E_\lambda)$ is the effective 'on-state' Hubbard U, and $L(E_\lambda)$ is the inverse participation ratio for TBM states of energy E_λ.

The interplay between disorder and interactions is directly evident here, for the greater the extent to which TBM states are localized (i.e. the larger $L(E_\lambda)$ is) the greater will be the enhancement of interactions, embodied in U_λ and acting to suppress double occupancy of pseudoparticle states. Equation (4.3) is formally similar to the true $V_{ij} = 0$ atomic limit of the disordered Hubbard model, but with $\epsilon_i \to E_\lambda$ and $U \to U_\lambda$. In the y regime, where it is qualitatively adequate, we expect behaviour strongly reminiscent of the true atomic limit, arising in essence from the combined effects of disorder and interactions [16, 22].

The extent to which such behaviour shows up in the present theory is illustrated in figures 2 and 3 for $y = 0.02$ (and $\tilde{U} = \frac{1}{2}, \tilde{\lambda} = \frac{1}{4}$). Figure 2($a$) shows the self-consistently determined $n(\epsilon)$ and $|\mu(\epsilon)|$ as a function of ϵ, the centre of $g(\epsilon)$ occurring at $\epsilon = 0$; these are contrasted with the atomic-limit results $|\mu(\epsilon)| = 1 = n(\epsilon)$ for $\epsilon < \epsilon_F^0(y)$ and zero otherwise, where the atomic-limit Fermi level $\epsilon_F^0(y)$ is shown. Figure 2(b) shows the Fermi-level charge distribution $H(\epsilon; E_F)$ (2.17), and the related $I(\epsilon) = g(\epsilon)n(\epsilon)/y$ giving the disorder-averaged ground-state charge density. Figure 3 shows the resultant total DOS, $D(E)$, which is contrasted with that for $U = 0$.

From figure 2 charge is indeed concentrated primarily on the small fraction of low-ϵ sites with $\epsilon \lesssim \epsilon_F^0(y)$, the slight tailing of $n(\epsilon)$ and $I(\epsilon)$ to higher ϵ reflecting a small contribution by such sites to occupied pseudoparticle states ($E < E_F(y)$ in $D(E)$), as discussed below.

In particular, figure 2(a) shows that significantly occupied sites with $\epsilon \lesssim \epsilon_F^0(y)$ have $|\mu(\epsilon)| \simeq n(\epsilon)$ and thus near maximum spin polarization. Since the mean site double-occupancy probability $P_2(\epsilon) = 0$ for sites with $|\mu(\epsilon)| = n(\epsilon)$ (2.19a), such sites can thus be at most singly occupied by an electron of a definite spin: the mean number of $-\sigma$-spin electrons on sites of energy ϵ that are preferentially occupied by σ-spin electrons, $n_{-\sigma}^{(\sigma)}(\epsilon) = \frac{1}{2}[n(\epsilon) - |\mu(\epsilon)|]$, vanishes when $|\mu(\epsilon)| = n(\epsilon)$. This is analogous to the true atomic limit where, for $\epsilon < \epsilon_F^0(y)$, $|\mu(\epsilon)| = n(\epsilon)(= 1)$. It is also commensurate with the arguments underlying (4.3), although the mean-field theory naturally cannot fully describe an extreme limit where the ground state consists of *strictly* non-overlapping singly occupied localized states: the latter implies $n_i = |\mu_i| > 0$ for sites that participate in any of the occupied pseudoparticle states, and $n_i = 0 = |\mu_i|$ for those that do not, with $P_{2i} = 0$ in each case and thus $P_2(\epsilon) = 0$ for all ϵ. While the mean-field theory can thus describe well the situation for $\epsilon < \epsilon_F^0(y)$, it will fail to account for the fact that a small fraction of the sites with a given $\epsilon > \epsilon_F^0$ will typically participate weakly in occupied pseudoparticle states ($n_i \ll 1$), whereas the majority of such sites will have $n_i = 0$. This is related to the fact that, for $\epsilon > \epsilon_F^0$, $|\mu(\epsilon)|$ drops below $n(\epsilon)$ and vanishes. Nonetheless, since $n(\epsilon) \ll 1$ here, $P_2(\epsilon)$ is very small so the mean-field result is not unduly awry.

In contrast to the true atomic limit, note next that although the vanishing of $P_2(\epsilon)$ when $|\mu(\epsilon)| = n(\epsilon)$ implies that a site of energy ϵ can only be singly occupied by an electron, it does not imply that such a site is inexorably occupied. With $P_2(\epsilon) = 0$, the mean probabilities that sites of energy ϵ are singly occupied, or empty, reduce respectively to $P_1(\epsilon) = n(\epsilon)$ and $P_0(\epsilon) = 1 - n(\epsilon)$. Only if $n(\epsilon) = 1$, as in the strict atomic limit, is $P_0(\epsilon) = 0, P_1(\epsilon) = 1$. From figure 2($a$) it is clear that $n(\epsilon) < 1$ for all significantly occupied sites, which therefore have a non-zero probability of being empty. This simply embodies the fact that while occupied pseudoparticle states at low y are mainly non-overlapping and singly occupied, they are not atomically localized

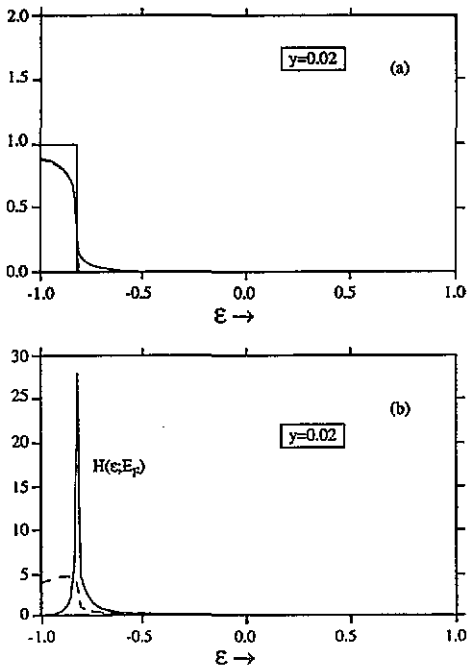

Figure 2. For $y = 0.02$, with $\tilde{U} = \frac{1}{2}$, $\tilde{\lambda} = \frac{1}{4}$. (*a*) $n(\epsilon)$ (full curve) and $|\mu(\epsilon)|$ (broken curve) against ϵ contrasted with the atomic limit result $n(\epsilon) = 1 = |\mu(\epsilon)|$ for $\epsilon < \epsilon_F^0(y)$. (*b*) The Fermi level charge distribution $H(\epsilon; E_F)$, and $I(\epsilon)$ (broken curve). All energies are in units of the zero-order bandwidth B.

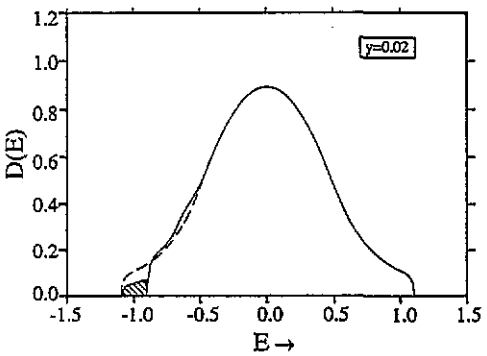

Figure 3. The self-consistent DOS, $D(E)$ (full curve) against E for $y = 0.02$, with $\tilde{U} = \frac{1}{2}$, $\tilde{\lambda} = \frac{1}{4}$. Occupied pseudoparticle states are shown shaded. The $U = 0$ non-interacting DOS is shown for comparison (broken curve).

on single sites. It is reflected further in the Fermi-level charge density $H(\epsilon; E_F)$ of figure 2(*b*) which, while sharply peaked at $\epsilon = \epsilon_F^0(y)$ indicating the dominance of such sites in Fermi-level states, has a small but non-vanishing width. Only in the atomic limit $B \to 0$ does $H(\epsilon; E_F)$ reduce to $\delta(\epsilon - \epsilon_F^0(y))$.

The quasiatomic behaviour at low y is also evident in $C(n)$ (2.18), with $C(n)\mathrm{d}n$ the mean fraction of sites with charge between n and $n + \mathrm{d}n$. For $y = 0.02$ in the true atomic limit, $C(n)$ reduces to $y\delta(n-1) + (1-y)\delta(n)$. Assuming, as found (figure 2(*a*)), that $n(\epsilon)$ is single-valued and monotonically decreasing in ϵ, whence the inverse function $\epsilon(n)$ is unique, (2.18) simplifies to

$$C(n) = \left|\frac{\mathrm{d}\epsilon(n)}{\mathrm{d}n}\right| g(\epsilon(n)) \tag{4.4}$$

so inspection of the gradient of $n(\epsilon)$ gives an indication of $C(n)$. In analogy with the true atomic limit, the $C(n)$ corresponding to figure 2(*a*) is found to be strongly peaked around $n \simeq 0$, with a smaller peak around $n \simeq 0.9$, and with virtually no weight in the intermediate range $0.1 \lesssim n \lesssim 0.9$.

Finally, the self-consistent total DOS, $D(E)$ (figure 3), also shows quasiatomic behaviour at low y. In the limit of strictly non-overlapping singly occupied localized

states, and because of the effective double exclusion principle that is thereby operative, it is straightforward to show [22] from the Hamiltonian (4.3) that for $E < E_F(y)$ the resultant $D(E)$ is one half of that for the $U = 0$ non-interacting limit, and that the $D(E)$ jumps discontinuously to the $U = 0$ DOS at $E = E_F+$. Such behaviour is qualitatively mirrored in figure 3 for the self-consistent $D(E)$ in comparison to the $U = 0$ limit (although, as mentioned above, the present theory cannot capture fully an extreme limit of strictly non-overlapping occupied states).

The broad physical picture of the low-y quasiatomic regime is thus of localized highly correlated electrons, evidenced in strong local charge accumulation on low-ϵ sites; strong spin localization; and a strong correlation between local charges and moments, with $|\mu(\epsilon)| \simeq n(\epsilon)$. This behaviour persists qualitatively up to a filling fraction of around $y_c \simeq 0.08$, the fraction of sites whose site energies lie below the lower band edge of the unperturbed $D_0(E)$ (figure 1(*a*)). For $y \gtrsim y_c$ however, a progressive deviation from the above picture occurs, as we now discuss.

4.2. *Intermediate regime:* $y_c \lesssim y < y_0$

Here we consider filling fractions up to $y = y_0$, where local moments are no longer stable; $y_0 \simeq 0.85$ with the chosen $\tilde{U} = \frac{1}{2}, \tilde{\lambda} = \frac{1}{4}$. As y is progressively increased above y_c, it is found in particular that the local charges and moments increasingly decorrelate, and sites in a narrowing ϵ-interval have progressively diminishing local moments.

We consider first $y = 0.15$, towards the lower end of the intermediate regime, although a smaller y would suffice. Figure 4(*a*) shows the resultant $n(\epsilon)$ and $|\mu(\epsilon)|$. These are contrasted with results for the atomic limit $B \to 0$. This consists of a small low-ϵ range of solely doubly occupied sites with $n(\epsilon) = 2, |\mu(\epsilon)| = 0$ extending up to $\epsilon = \epsilon_F^0(y) - U$; a singly occupied ϵ-interval with $n(\epsilon) = 1 = |\mu(\epsilon)|$ extending from $\epsilon_F^0 - U$ up to ϵ_F^0 (whose width U reflects stability of the atomic limit ground state against particle–hole excitations); and solely empty sites for $\epsilon > \epsilon_F^0(y)$. Figure 4(*a*) shows that significant erosion of atomic-limit behaviour has begun to occur. The moments are weakening and are appreciable in an ϵ-range noticeably less than U in width. More importantly, $|\mu(\epsilon)| < n(\epsilon)$ for all ϵ, so even sites with appreciable local moments, which are mainly singly occupied by electrons and preferentially associated with one spin type, σ, have $P_2(\epsilon) > 0$ and thus a significant probability of being occupied also by $-\sigma$-spin electrons: $n_{-\sigma}^{(\sigma)}(\epsilon) = \frac{1}{2}[n(\epsilon) - |\mu(\epsilon)|] > 0$. In contrast to the quasiatomic y-regime, this reflects not inappreciable overlap of the occupied pseudoparticle states.

Figure 4(*b*) shows the corresponding $H_\sigma(\epsilon; E_F)$ for $y = 0.15$, the vertical scale of which is an order of magnitude below that for figure 2(*b*). Note first that sites with the strongest moments give only a minor contribution to the charge density in Fermi-level states, in agreement with the SIAM parallel of section 3; and also that $n(\epsilon_m)$ for sites on which moments are a maximum is indeed close to unity, $n(\epsilon_m) \simeq 0.91$.

Secondly, and again similarly to the SIAM [24], sites with bare site energies reasonably close to the upper (lower) local moment boundary are found to have an effective σ-spin site energy $\epsilon_\sigma^{(\sigma)}$ ($\epsilon_\sigma^{(-\sigma)}$) lying within a relatively small width of E_F: such sites thus naturally participate significantly in the Fermi-level charge distribution $H_\sigma(\epsilon; E_F) \propto D_\sigma(\epsilon; E_F)$. In particular, the lower peak in $H_\sigma(\epsilon; E_F)$ arises from low-ϵ sites close to the lower local moment boundary that have a significant probability of being occupied by electrons (and thus an appreciable charge) and which, when

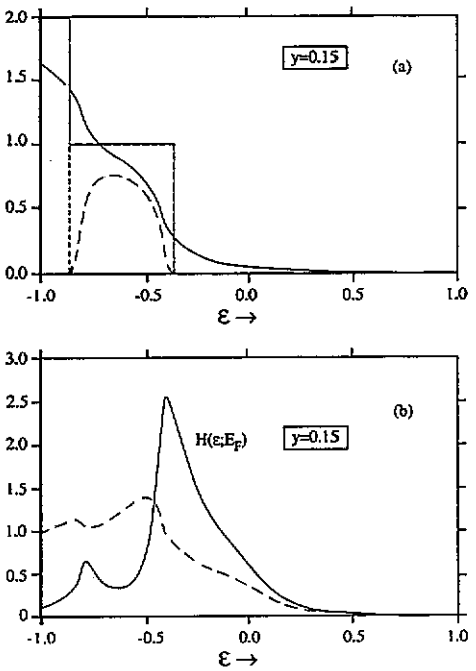

Figure 4. As for figure 2 but for $y = 0.15$. The atomic limit for $n(\epsilon)$ ($|\mu(\epsilon)|$) in figure 4(a) is shown by a full (dotted) curve. Note that the vertical scale of figure 4(b) is an order of magnitude lower than that for figure 2(b).

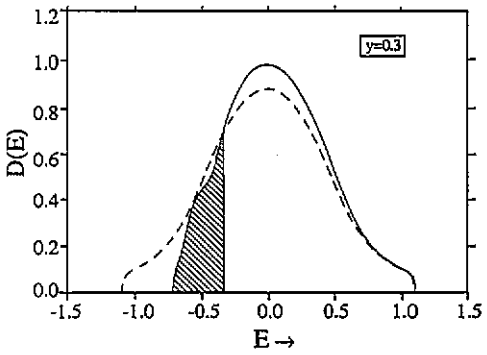

Figure 5. As for figure 3 but for $y = 0.3$.

occupied, are preferentially occupied by $-\sigma$-spin electrons: the mean number of $-\sigma$-spin electrons on such sites, $n_{-\sigma}^{(-\sigma)}(\epsilon) = \frac{1}{2}[n(\epsilon) + |\mu(\epsilon)|]$, is thus somewhat less than, but of order, unity. Hence the effective site energy for a σ-spin electron incident upon such sites, $\epsilon_\sigma^{(-\sigma)} = \epsilon + U n_{-\sigma}^{(-\sigma)}(\epsilon)$ is close to $\epsilon + U$; so sites with bare ϵ somewhat less than but of order U below E_F thus participate significantly in Fermi-level states. In contrast, the upper peak in $H_\sigma(\epsilon; E_F)$ arises from sites close to the upper local moment boundary that have only a modest probability of being occupied (and thus a modest charge) and which, if possessing moments, are preferentially occupied by σ-spin electrons; thus the effective site energy for a σ-spin electron incident upon such sites, $\epsilon_\sigma^{(\sigma)} = \epsilon + U n_{-\sigma}^{(\sigma)}(\epsilon)$ with $n_{-\sigma}^{(\sigma)}(\epsilon) = \frac{1}{2}[n(\epsilon) - |\mu(\epsilon)|]$, is only slightly in excess of the bare ϵ. Sites for which ϵ is close to E_F thus contribute significantly to the Fermi-level charge density.

With increasing filling fraction, the deviation from atomic or quasiatomic behaviour becomes increasingly pronounced. The pseudoparticle spectrum $D(E)$ is no longer simply related to that for $U = 0$, to which it is compared in figure 5 for $y = 0.3$. That progressively weakening local moments exist in an ϵ-interval, which becomes steadily smaller than the atomic limit width U, is clear from figure 4(a) (for $y = 0.15$) and figure 6(a) ($y = 0.6$), and is also reflected in decreasing separation between the peaks of $H_\sigma(\epsilon; E_F)$ as y increases. Moreover, the peaks broaden and

ultimately lose their identity: their widths are essentially proportional to $D(E_F)$ (see (3.3)) which increases progressively with filling fraction as $E_F(y)$ moves further into the band.

In contrast to the quasiatomic y-regime where the Fermi-level charge distribution is sharply distributed on a small fraction of low-ϵ sites (figure 2(b)), $H_\sigma(\epsilon; E_F)$ in the intermediate y-domain is clearly distributed over a much larger fraction of available sites. In addition, as seen from figures 4(b) and 6(b), the dominant contribution to $H_\sigma(\epsilon; E_F)$ shifts to sites with increasingly higher ϵ as y is increased, tending towards the maximum in the site energy distribution at $\epsilon = 0$: for both $y = 0.3$ and 0.6, for example, electrons in pseudoparticle states at E_F are most probably found on sites within $\pm\tilde{\lambda}$ of $\epsilon = 0$ (with $\tilde{\lambda}$ the halfwidth of $g(\tilde{\epsilon})$).

This is qualitatively significant for the transition from insulating to metallic behaviour, which will occur at the filling fraction y_m where pseudoparticle states at E_F become extended. Although we emphasize that localization characteristics are not directly addressed by the present theory, the tendency to delocalization of Fermi-level pseudoparticle states is clearly enhanced as the corresponding charge distribution becomes significantly distributed over sites with $\epsilon \simeq 0$ close to the maximum in $g(\epsilon)$, such sites typically being surrounded by sites whose σ-spin site energy difference is small compared to the transfer matrix elements that connect them. Further, the probability density of σ- spin site energies, $F(\epsilon_{i\sigma})$ $(= F(\epsilon_{i-\sigma}))$, is given (2.5),(2.8) by

$$F(\epsilon_{i\sigma}) = \int_{-\infty}^{\infty} \tfrac{1}{2}[\delta(\epsilon_{i\sigma} - \epsilon_\sigma^{(\sigma)}(\epsilon)) + \delta(\epsilon_{i\sigma} - \epsilon_\sigma^{(-\sigma)}(\epsilon))]g(\epsilon)\mathrm{d}\epsilon \qquad (4.5)$$

with $\epsilon_\sigma^{(\pm\sigma)} = \epsilon + \frac{1}{2}U[n(\epsilon) \mp |\mu(\epsilon)|]$. Consideration of $n(\epsilon)$ and $|\mu(\epsilon)|$ for $y = 0.3$ or $y = 0.6$ (figure 6(a)) shows the resultant $F(\epsilon_{i\sigma})$ to be narrower, by an amount of order $\tilde{U}$ $(= \frac{1}{2})$, than its corresponding $U = 0$ limit, $g(\epsilon)$, due mainly to significant electron double-occupancy of low-ϵ sites. The disorder in the σ-spin site energies is thus, in effect, less than that for the non-interacting limit, which should act *per se* to stabilize the metallic phase as found by Singh [13], Ma [15] and Logan and Tusch [25] in studies of a half-filled site-disordered Hubbard model.

Aside from these qualitative remarks we clearly cannot specify the insulator–metal filling fraction, y_m, except that $y_m > y_c$ is naturally expected because the physical picture of the quasiatomic regime is of primarily non-overlapping singly occupied localized states, significant erosion of which will begin when the occupied states are still localized. We add, however, that numerical studies [26] at full UHF level indicate that states at E_F delocalize at a y_m in the intermediate y-regime where local moments still persist. Milovanović and co-workers [11] also find simultaneous coexistence of delocalized states at E_F, and local moments, in their work on a spatially disordered Hubbard model.

4.3. Non-magnetic regime: $y_0 < y \leqslant 1$

For $y = 0.6$ (figure 6) the local moments on sites in a small ϵ-range are already weak, although feeble moments persist up to $y = y_0 \simeq 0.85$ with $\tilde{U} = \frac{1}{2}, \tilde{\lambda} = \frac{1}{4}$. Above y_0 the system cannot support local moments, with implications discussed further in section 5.

As an example, figure 7 shows $n(\epsilon)$ and $H_\sigma(\epsilon; E_F)$ for half-filling $y = 1$; the corresponding total DOS is shown in figure 8(a). Here we simply note that for the

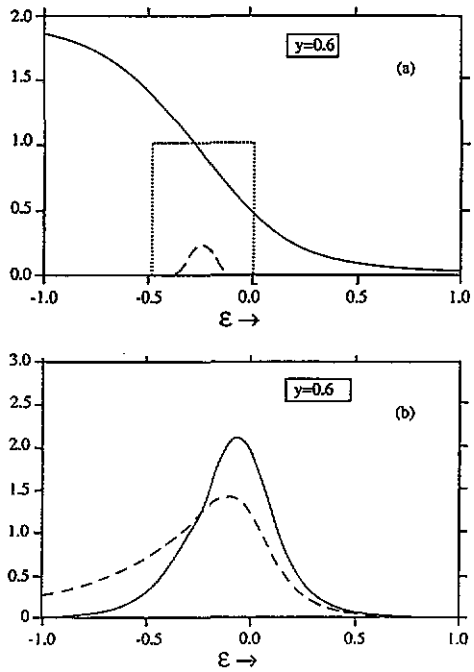

Figure 6. As for figure 2 but for $y = 0.6$. Only the atomic limit $|\mu(\epsilon)|$ (dotted line) is shown. Again note the order of magnitude reduction from figure 2(*b*) in the vertical scale of figure 6b

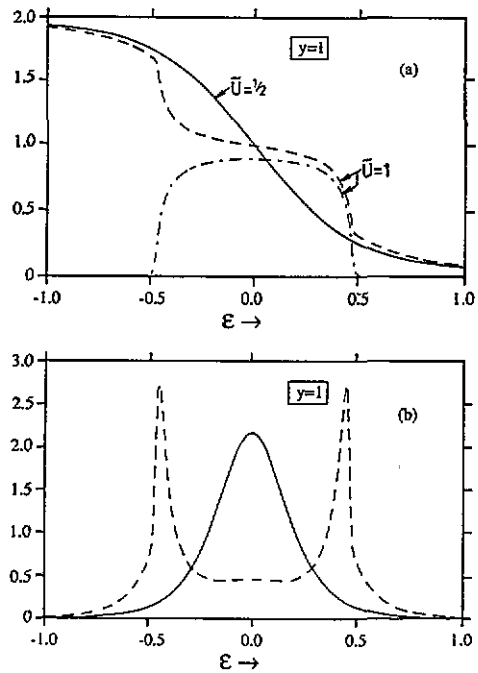

Figure 7. For $y = 1$, with $\tilde{\lambda} = \frac{1}{4}$. (*a*) $n(\epsilon)$ (full curve) for $\tilde{U} = \frac{1}{2}$ where no moments are stable at half-filling; and $n(\epsilon)$ (broken curve), $|\mu(\epsilon)|$ (chain curve) for $\tilde{U} = 1$. (*b*) Corresponding $H(\epsilon; E_F)$ for $\tilde{U} = \frac{1}{2}$ (full curve) and $\tilde{U} = 1$ (broken curve).

non-magnetic regime, the SIAM parallel of section 3 predicts $H(\epsilon; E_F)$ to receive a significant contribution from sites of energy ϵ for which $n(\epsilon) \simeq 1$, whose effective site energies $\epsilon + \frac{1}{2}Un(\epsilon)$ are close to E_F. This is clearly seen in figures 7 and 8: the broadly distributed $H(\epsilon; E_F)$ of figure 7(*b*) for $\tilde{U} = \frac{1}{2}$ is symmetric in ϵ about $\epsilon = 0$, for which (from figure 7(*a*)) $n(0) = 1$. From figure 8(*a*), the Fermi level E_F indeed lies precisely at $\frac{1}{2}U$ ($E_F/B = \frac{1}{4}$).

5. The role of $\tilde{U}$

In section 4 we considered fixed $\tilde{U} = \frac{1}{2}$ and $\tilde{\lambda} = \frac{1}{4}$. Here we first discuss the dependence of results on the scaled interaction strength $\tilde{U} = U/B$, retaining $\tilde{\lambda} = \frac{1}{4}$ for the scaled disorder measure. As $\tilde{U}$ progressively increases, moments naturally persist to higher filling fractions, and $y_0 = 1$ for $\tilde{U} \sim 0.55$, above which the non-magnetic y-regime is eliminated and moments exist at half-filling.

Figures 7 and 8(*b*) are for $\tilde{U} = 1$ at half-filling, $y = 1$. The DOS (figure 8(*b*)) has a pronounced pseudogap centred on $E = E_F$, reflecting the occurrence of strong local moments (figure 7(*a*)) on sites in an ϵ-range of width somewhat less than U. As $\tilde{U}$ is further increased the pseudogap deepens, and for $\tilde{U} \gtrsim 2$ a Hubbard gap

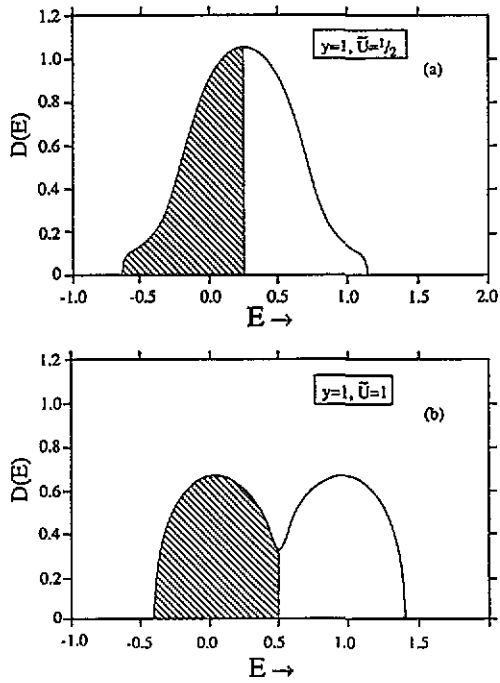

Figure 8. The self-consistent DOS $D(E)$ at half-filling, $y = 1$, with $\tilde{\lambda} = \frac{1}{4}$ and (a) $\tilde{U} = \frac{1}{2}$, (b) $\tilde{U} = 1$. Energies are in units of the zero-order ($U = 0 = \lambda$) bandwidth B.

(centred on $E_F = \frac{1}{2}U$) occurs in $D(E)$—as expected from the atomic limit where a true Hubbard gap occurs in the single-particle spectrum $D(E)$ only for U in excess of the full width $2\epsilon_U$ of the site energy distribution $g(\epsilon)$ (i.e. $\tilde{U} > 2$ here).

Regarding the SIAM parallel (section 3), figures 7(a) and (b) for $\tilde{U} = 1$ show that sites with strong moments give only a minor contribution to the Fermi-level charge distribution; in contrast, $H_\sigma(\epsilon; E_F)$ is strongly dominated by sites with bare site energies close to the local moment boundaries, whose effective σ-spin site energies are close to E_F. In addition, sites with $\epsilon_m = 0$ for which moments are maximum indeed have $n(\epsilon_m) = 1$, with E_F lying exactly midway between the corresponding σ-spin site energies $\epsilon_{\pm\sigma}^{(\sigma)}(\epsilon)$, namely $E_F = \frac{1}{2}B = \epsilon_m + \frac{1}{2}Un(\epsilon_m)$, see figure 8($b$).

Using (4.4), comparison of the gradients of $n(\epsilon)$ for the $\tilde{U} = \frac{1}{2}$ and 1 cases of figure 7(a) also shows the strong suppression of charge fluctuations as $\tilde{U}$ is increased, embodied in the probability density $C(n)$ that any site picked at random will have a local charge n: in contrast to the broad $C(n)$ distribution resulting for $\tilde{U} = \frac{1}{2}$, $C(n)$ for $\tilde{U} = 1$ is very sharply distributed around $n = 1$ with a halfwidth $\Delta n \sim 0.1$, and charge fluctuations are thus of minor importance.

The comments above refer to $y = 1$, but of greater significance here is the differential influence of $\tilde{U}$ on local moment stability for different filling fractions. At half-filling, $y = 1$, we have seen that there are no moments for $\tilde{U} = \frac{1}{2}$, but that weak moments occur with $\tilde{U}$ increased to, say, 0.6. In contrast, for the quasiatomic regime $y \lesssim y_c = 0.08$, strong atomic-like moments on the small fraction of significantly

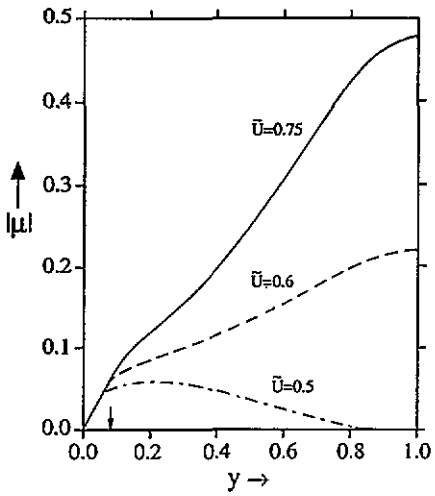

Figure 9. The mean magnitude of the local moment per site, $|\mu|$, against filling fraction y, with $\tilde{\lambda} = \frac{1}{4}$ and for $\tilde{U} = 0.5$, 0.6 and 0.75. $y_c = 0.082$ is indicated by an arrow.

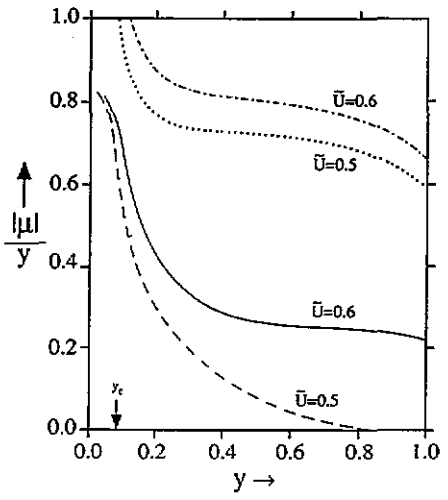

Figure 10. The mean magnitude of the local moment per electron, $|\mu|/y$, against filling fraction y, with $\tilde{\lambda} = \frac{1}{4}$ and for $\tilde{U} = 0.5$ (broken curve), $\tilde{U} = 0.6$ (full curve). Corresponding atomic limit results are also shown: dotted curve, $\tilde{U} = 0.5$; chain curve, $\tilde{U} = 0.6$.

occupied low-ϵ sites are evident for $\tilde{U} = \frac{1}{2}$ (figure 2(*a*)).

To illustrate this we consider first the mean local moment magnitude per site, $|\mu| = \langle N_s^{-1} \sum_i |\mu_i| \rangle$, given by

$$|\mu| = \int_{-\infty}^{\infty} |\mu(\epsilon)| g(\epsilon) \mathrm{d}\epsilon. \tag{5.1}$$

Figure 9 shows $|\mu|$ against y for $\tilde{U} = 0.5, 0.6$ and 0.75. In the quasiatomic regime $y \lesssim y_c$, increasing $\tilde{U}$ above $\frac{1}{2}$ produces virtually no change in $|\mu|$, which is essentially linear in y. In contrast, for y in excess of y_c, and for $y \simeq 1$ in particular, increasing $\tilde{U}$ is seen to have a pronounced effect on the existence and stability of local moments. The characteristics of the quasiatomic regime are, however, recovered as y is decreased below $\sim y_c$, regardless of whether local moments exist around half-filling. This is to be expected, despite the common view that half-filling $y = 1$ is optimal for local moment formation: as y is decreased and E_F thus moves progressively towards the lower edge of $D(E)$, occupied pseudoparticle states are increasingly dominated by low-ϵ sites, and their localization will eventually lead to a strong enhancement of interaction effects, resulting in the occurrence of the quasiatomic domain described in section 4.1. The essential independence of $|\mu|$ on $\tilde{U}$ in the latter regime is also natural, for provided $\tilde{U}$ is sufficiently large to ensure an effective double exclusion principle leading to mainly singly occupied non-overlapping pseudoparticle states, a further increase in $\tilde{U}$ will not appreciably change the occupancy of the states. As we have seen, however, what is in effect an infinite value of $\tilde{U}$ at low filling may not be sufficient to secure even the existence of moments around half-filling.

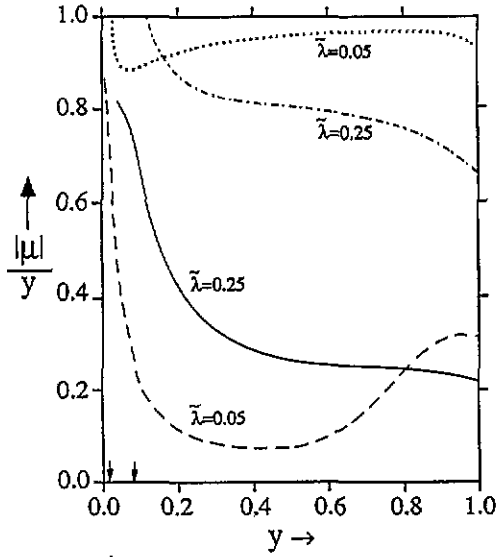

Figure 11. The mean magnitude of the local moment per electron, $|\mu|/y$, against filling fraction y, for $\tilde{U} = 0.6$ and $\tilde{\lambda} = 0.05$ (broken curve), $\tilde{\lambda} = 0.25$ (full curve). Corresponding atomic limit results are also shown. The y axis arrows show $y_c = 0.016$ (for $\tilde{\lambda} = 0.05$) and $y_c = 0.082$ (for $\tilde{\lambda} = 0.25$).

To highlight the above, figure 10 shows the mean magnitude of the local moment *per electron*, $\langle N_e^{-1} \sum_i |\mu_i| \rangle = |\mu|/y$, for $\tilde{U} = 0.5$ and 0.6, weak moments existing in the latter case at half-filling. The corresponding atomic limit results $|\mu|/y = y_s/y$ (with y_s the fraction of singly occupied sites) are also shown: strong moments clearly occur for all y in the true atomic limit, the slow decrease in $|\mu|/y$ reflecting an increase in the fraction y_d ($= \frac{1}{2}[y - y_s]$) of doubly occupied diamagnetic sites as y increases towards half-filling. Strong erosion of atomic-limit behaviour is evident in $|\mu|/y$ for most of the y-range, but as the filling fraction is progressively decreased $|\mu|/y$ increases to a value somewhat less than one for $y \lesssim y_c$ in the quasiatomic regime. In fact, as in section 4.1, were the present theory able to describe fully a limit of strictly non-overlapping pseudoparticle states, we would have $n_i = |\mu_i|$ for all sites i, and thus $|\mu|/y = 1$ in this case even though the occupied sites are not atomically localized.

We mention also the effect at low y of decreasing $\tilde{U}$. In the strict atomic limit, sites are singly occupied only for a filling fraction up to y' such that the atomic limit Fermi level $\epsilon_F^0(y') = \epsilon_L + U$ (with ϵ_L the lower edge of $g(\epsilon)$); and for $y > y'$ double occupancy of low-ϵ sites occurs. This leads simply to $|\mu| = y$ for $y < y'$ and $|\mu| = y_s$ for $y > y'$ as seen in the atomic limit results of figure 10. The fraction of sites whose site energies lie below the lower edge at $-\frac{1}{2}B$ of the unperturbed $D_0(E)$ (figure 1(a)) is $y_c = 0.08$, and for $U < [-\frac{1}{2}B - \epsilon_L]$ (i.e. $\tilde{U} < \frac{1}{2}$ in the present calculations) double occupancy of low-ϵ sites will begin at a filling fraction $y' < y_c$. This is naturally reflected in the resultant $n(\epsilon)/|\mu(\epsilon)|$ from the mean-field theory: the quasiatomic regime of mainly singly occupied non-overlapping states then obtains for $y \lesssim y'$, although significant erosion of atomic-like behaviour again does not occur until $y \gtrsim y_c$.

Finally, we comment briefly on the role of the halfwidth $\tilde{\lambda}$ of the site energy distribution $g(\epsilon)$. As $\tilde{\lambda}$ is reduced, y_c decreases (equation (4.1) and figure 1(a)): with $\tilde{\lambda} = 0.05$, for example, $y_c \simeq 0.016$. The quasiatomic y-regime thus becomes smaller in extent. Further, the diminution of site disorder with decreasing $\tilde{\lambda}$, coupled with the fact that sites with ϵ well within the unperturbed bandwidth will in effect be accessed at smaller filling fractions, would suggest a relative reduction in local moment stability as y is initially increased beyond the quasiatomic regime. To illustrate this, figure 11 shows the mean moment magnitude per electron, $|\mu|/y$, for fixed $\tilde{U} = 0.6$ (where weak moments occur at half-filling) with $\tilde{\lambda} = \frac{1}{4}$ and 0.05. As y increases above $\sim y_c$ it is indeed found that $|\mu|/y$ drops more rapidly for $\tilde{\lambda} = 0.05$, indicating a relative reduction in local moment stability for smaller site disorder. We also note that, for the $\tilde{\lambda} = 0.05$ example, $y \simeq 1$ is optimal for local moment formation in the sense that as the filling fraction is reduced below half-filling, $|\mu|/y$ (as well as $|\mu|$ itself) initially decreases; but as y is decreased further towards $\sim y_c$ the characteristic signature of the quasiatomic regime is again naturally recovered.

6. Conclusion

A statistical mean-field treatment of a disordered Hubbard model at a UHF level has been developed. The essential element of the theory is the use of the site energies, ϵ, as a 'window' on local environments that lead to inhomogeneity in the distribution of local charges and magnetic moments; these, together with relevant total and local pseudoparticle spectra, were determined self-consistently at a CPA level. The resultant interplay between disorder and electron interactions was evident in particular in the evolution of the system with filling fraction (section 4) for a fixed (weak coupling) value of the scaled interaction strength $\tilde{U}$ and a given scaled disorder $\tilde{\lambda}$; and also in the differential effect of $\tilde{U}$ on local moment stability for different filling fractions (section 5). Further, despite the undoubted simplicity of the present mean-field theory, the perspective it suggests is supported by detailed computational studies of a site-disordered Hubbard model at UHF level, for both half-filling $y = 1$ [25,26] and as a function of y [26]: localization characteristics, and electronic properties of the system such as those we have considered, are found to be quite insensitive to magnetic ordering (long ranged or local) of the moments, and the parallel with the single impurity Anderson model discussed here (sections 3–5) is amply confirmed.

Acknowledgments

FS acknowledges the award of a Fellowship from the Italian CNR. We are grateful to many people for helpful discussions, and to M A Tusch in particular. The helpful suggestions of a referee are also gratefully acknowledged.

References

[1] Lee P A and Ramakrishnan T V 1985 *Rev. Mod. Phys.* **57** 287
[2] Efros A L and Pollack M 1985 *Electron–Electron Interactions in Disordered Systems* (Amsterdam: North-Holland)

[3] Kamimura H and Aoki H 1989 *The Physics of Interacting Electrons in Disordered Systems* (Oxford: Clarendon)
[4] Abrahams E, Anderson P W, Lee P A and Ramakrishnan T V 1981 *Phys. Rev.* B **24** 6783
[5] Finkelstein A M 1983 *Sov. Phys.–JETP* **57** 97
[6] Castellani C, DiCastro C, Lee P A and Ma M 1984 *Phys. Rev.* B **30** 527
[7] Castellani C, Kotliar B G and Lee P A 1986 *Phys. Rev. Lett.* **56** 1179
[8] Belitz D and Kirkpatrick T 1989 *Phys. Rev. Lett.* **63** 1296
[9] Sachdev S 1989 *Phys. Rev.* B **39** 5297
[10] Dasgupta C and Halley J W 1993 *Phys. Rev.* B **47** 1126
[11] Milovanović M, Sachdev S and Bhatt R N 1989 *Phys. Rev. Lett.* **63** 82
[12] Zimanyi G T and Abrahams E 1990 *Phys. Rev. Lett.* **64** 2719
[13] Singh A 1988 *Phys. Rev.* B **37** 430
[14] Shimizu A, Aoki H and Kamimura H 1986 *J. Phys. C: Solid State Phys.* **19** 725
[15] Ma M 1982 *Phys. Rev.* B **26** 5097
[16] Kamimura H 1980 *Phil. Mag.* B **42** 763
[17] Aoki H and Kamimura H 1976 *J. Phys. Soc. Japan* **40** 6
[18] Logan D E 1991 *J. Chem. Phys.* **94** 628
[19] Cyrot M 1972 *Phil. Mag.* **25** 1031
[20] Siringo F and Logan D E 1991 *J. Phys.: Condens. Matter* **3** 4747
[21] Hensel F 1979 *Adv. Phys.* **28** 555
[22] Logan D E and Siringo F 1992 *J. Phys.: Condens. Matter* **4** 3695
[23] Economou E N, White C T and de Marco R R 1978 *Phys. Rev.* B **18** 3946, 3968
[24] Anderson P W 1961 *Phys. Rev.* **124** 41
[25] Logan D E and Tusch M A 1993 *J. Non-Cryst. Solids* (in press)
[26] Tusch M A and Logan D E 1993 to be submitted
[27] Logan D E and Winn M D 1988 *J. Phys. C: Solid State Phys.* **21** 5773
[28] Soven P 1967 *Phys. Rev.* **156** 809
[29] Velicky B, Kirkpatrick S and Ehrenreich H 1968 *Phys. Rev.* **157** 747
[30] Roth L M 1974 *J. Physique* **35** C4-317; 1974 *Phys. Rev.* B **9** 2476
[31] Winn M D and Logan D E 1989 *J. Phys.: Condens. Matter* **1** 1753
[32] Economou E N 1983 *Green's Functions in Quantum Physics* (Berlin: Springer)
[33] Paalanen M A, Graebner J, Bhatt R N and Sachdev S 1988 *Phys. Rev. Lett.* **61** 597
[34] Münster P and Freyland W 1979 *Phil. Mag.* **39** 93